Polyhedron 27 (2008) 2379–2385

Contents lists available at ScienceDirect

Polyhedron

journal homepage: www.elsevier.com/locate/poly

Ring opening complexation of nickel(II) and copper(II) by 2-phenyl-2-(2-pyridyl)imidazolidine: Synthesis, spectra and X-ray crystal structures

Sanaa M. Emam [a,1], Patrick McArdle [a,*], James McManus [b], Mary Mahon [b]

[a] Chemistry Department, National University of Ireland, Galway, Ireland
[b] Chemistry Department, University of Bath, UK

ARTICLE INFO

Article history:
Received 7 February 2008
Accepted 10 April 2008
Available online 4 June 2008

Keywords:
Schiff base
Azide
X-ray crystal structure
DFT calculations
Nickel(II)
Copper(II) complexes

ABSTRACT

The cyclic structure of 2-phenyl-2-(2-pyridyl)imidazolidine (**1**) derived from the condensation of 1,2-diaminoethane and 2-benzoylpyridine has been confirmed by X-ray crystallography. Reaction of (**1**) with salts of nickel(II) and copper(II) leads to metal induced ring opening and the formation of complexes containing the tridentate ligand (L). The formulae of the complexes derived from NiX_2 and CuX_2 are $[NiL_2]X_2$ and $[CuLY]X_2$ (X=ClO_4^-, Y = H_2O, CH_3CN and N_3^-). Crystal structures were obtained for (**1**), $[NiL_2][ClO_4]_2$, $[CuL(CH_3CN)][ClO_4]_2$, $[CuL(H_2O)][NO_3]_2$ and $[CuLN_3][ClO_4]$.

1. Introduction

Schiff base ligands have played an important role in our understanding of the coordination chemistry of transition metal ions and Schiff base complexes have a broad range of applications including, enzyme inhibition [1], anti-microbial action [2] and catalytic activity when encapsulated in zeolite Y [3]. In this paper, the imidazoline (**1**), the result of a disfavoured 5-*Endo-Trig* cyclization [4], is reacted with nickel and copper salts to yield tridentate complexes. The structures of the complexes which could be crystallized and analysed by X-ray diffraction are discussed. Prompted by reports of the use of DFT calculations in modeling nickel and copper complexes, with similar and greater complexity than those described here [5,6], it has been found that while calculations for the nickel system reproduced the details of the crystallographic results the copper results were less satisfactory.

2. Experimental

2.1. Chemicals and materials

2-Benzoylpyridine and 1,2-diaminoethane (from Sigma–Aldrich and BDH) were used without further purification. Sodium azide (Sigma–Aldrich), $Ni(ClO_4)_2 6H_2O$ (Sigma–Aldrich), $Cu(ClO_4)_2 6H_2O$ (Aldrich), $Ni(NO_3)_2 6H_2O$ (Merck) and $Cu(NO_3)_2 4H_2O$ (Riedel de-Haen) were used as received. All other chemicals and solvents were AR grade and used as received. Ethanol was dried prior to use.

2.2. Instrumentation

Elemental analyses (carbon, hydrogen and nitrogen) were carried out on a Perkin–Elmer 240 CHN elemental analyzer. IR spectra were measured on a Perkin–Elmer Spectrum One Diamond-ATR-FT-IR instrument spectrometer, UV–Vis spectra were recorded using a Varian Cary 50 spectrometer using 1 cm quartz cuvettes. ^1H and ^{13}C NMR spectra were recorded on a JEOL ECX-400 NMR spectrometer at room temperature with tetramethylsilane as internal reference. Magnetic moments were measured on a Sherwood Scientific magnetic susceptibility balance at room temperature. The diamagnetic corrections were calculated by using Pascal's constants and $Hg[Co(SCN)_4]$ was used as a calibrant. Molar conductivities were measured using freshly prepared 10^{-3} M solutions in nitromethane, acetonitrile and dimethylformamide at

* Corresponding author.
E-mail address: p.mcardle@nuigalway.ie (P. McArdle).
[1] Permanent address: Chemistry Department, Faculty of Science, El-Menoufia University, Shebin El-Kom, Egypt.

0277-5387/$ - see front matter © 2008 Elsevier Ltd. All rights reserved.
doi:10.1016/j.poly.2008.04.028

room temperature, using a Jenway 4310 conductivity meter and the cell constant was calibrated with 0.01 M KCl solution. Melting points were measured using a Gallenkamp melting point apparatus.

2.3. Synthesis of 2-phenyl-2-(2-pyridyl)imidazolidine (**1**)

The ligand 2-phenyl-2-(2-pyridyl) imidazolidine was prepared using a slight variation of the procedure reported in the literature [7]. An anhydrous ethanol solution (15 cm^3) of 2-benzoylpyridine (8.0 g, 0.04 mol), was treated dropwise with 1,2-diaminoethane (2.62 g, 0.05 mol) in the same solvent (5.0 cm^3) with constant stirring and the mixture was then heated under reflux for 16 h. The yellow solution was concentrated under reduced pressure, cooled and the formed faint yellow precipitate filtered. The product was re-crystallized from *n*-hexane giving almost colourless crystals, melting point is (83–85 °C). *Anal.* Calc. for $C_{14}H_{15}N_3L$: C, 74.63; H, 6.7; N, 18.67. Found: C, 74.81; H, 6.47; N, 18.46%. IR (Diamond ATR cm^{-1}): υ(N–H) 3320, 3247 (broad); υ(C=N) 1620, 1538, 1567, υ(C=C) 1490 1448, 1425. ^1H NMR data in $CDCl_3$ at 298 K: δ (ppm): 8.73 d(1) (H_6); 8.5 t(1) (H_4); 7.95 m(1) (H_5); 7.69 d(1) (H_3); 7.57–7.42 m(5) (H_{13}–H_{17}); 3.05 m(2) (H_{10}); 2.99 m(2) (H11); 2.82 br(2) (H 7, 9).^{13}C NMR in $CDCl_3$: δ (ppm): 163.3 (C-2); 150.2 (C6); 144.2 (C12); 136.7 (C4); 128.28 (C14, 16); 127.1 (C13, 17); 122.1 (C15); 85.9 (C8); 46.3(C10,11); UV–Vis (CH_3CN): λ_{max} 290, 275 and 252 nm.

2.4. Preparation of metal complexes, L= (**1**)

2.4.1. [Ni(L)$_2$][ClO$_4$]$_2$ (**2**)

To a stirred solution of (**1**) (1.0 g, 0.004 mol) in acetonitrile (7 cm^3), a solution of $Ni(ClO_4)_2 \cdot 6H_2O$ (1.6 g, 0.004 mol) in the same solvent (7 cm^3) was added dropwise with constant stirring. The solution colour changed from yellow to a dark red. The reaction mixture was stirred at room temperature for 3 h and left to stand overnight. Evaporation of the solvent left a toffee like residue. This was dissolved in warm methanol from which red crystals were obtained. *Anal.* Calc. for $C_{28}H_{30}N_6Cl_{I2}NiO_8$ (**2**): C, 47.48; H, 4.23; N, 11.86. Found: C, 47.49; H, 4.07; N, 12.21%. Λ_M (Ω^{-1} cm^2 mol^{-1}) in CH_3CN and CH_3NO_2: 275 and 156. IR (Diamond ATR cm^{-1}): υ(N–H) 3342, 3293 (broad, m); 1646 υ(C=N); 1595, 1580 υ(C=C), υ(C=N)$_{py}$, δ(N–H), υ(ClO_4) 1070; UV–Vis (CH_3CN; λ_{max}):784, 531, 464 nm. μ_{eff} (BM): 3.34.

The red crystals were re-crystallized from a chloroform methanol mixture to give a second crop of red crystals of formula $C_{28}H_{30}N_6Cl_{I2}NiO_8 \cdot CHCl_3$ which were suitable for crystallography.

2.4.2. [Ni(L)(N$_3$)$_2$DMF] (**3**)

The ligand (**1**) (1.0 g, 0.004 mol) was dissolved in absolute ethanol (5 cm^3) and a solution of $Ni(ClO_4)_26H_2O$ (1.6 g, 0.004 mol) in ethanol (7 cm^3) was added drop-wise with constant stirring. The yellow colour of the solution changed to a dark red with the formation of a semi-solid mass. Rapid stirring for one hour led to the formation of a solid which was treated with a hot methanolic solution (15 cm^3) of NaN_3 (1.2 g, 0.016 mol). The reaction mixture was stirred for 4 h and a buff precipitate formed. This was left to stand for 24 h and then stirred for 2 h, filtered and the filtrate was dissolved in hot acetonitrile filtered concentrated and allowed to cool to room temperature yielding yellowish brown micro crystals. These crystals were dissolved in DMF and re-crystallized by vapour diffusion of diethyl ether from an adjacent container. This afforded dark brown crystals (melting point 195 °C) which were not suitable for crystallography. *Anal.* Calc. for $C_{17}H_{22}N_{10}ONi$: C, 46.28; H, 5.02; N, 31.75. Found: C, 45.35; H, 4.08; N, 33.91%. Λ_M (S cm^2 mol^{-1}) in DMF: 23.0. IR (cm^{-1}): υ(N–H) 3312, 3247, 3153; υ(N_3) 2020; υ(C=N) 1650; υ(C=C), υ(C=N)$_{py}$, δ(N–H), 1589, 1570. UV–Vis (DMF. λ_{max}): 690, 522, 463 nm. μ_{eff} (BM): 3.30.

2.4.3. [Cu(L)(CH$_3$CN)][ClO$_4$]$_2$ (**4**)

To a stirred solution of (**1**) (1.0 g, 0.004 mol) in absolute ethanol (6 cm^3), a solution of $Cu(ClO_4)_2 \cdot 6H_2O$ (1.6 g, 0.004 mol) in acetonitrile (3 cm^3) was added dropwise with constant stirring. The colour changed from yellow to green and then to blue as the copper perchlorate solution was added. The reaction mixture was stirred for 5 h at room temperature and a blue precipitate formed. It was isolated by filtration, washed with a mixture of ethanol and acetonitrile and dried under vacuum. Crystals grown from acetone solution were of poor quality however crystallization from a mixture of acetonitrile and ethanol afforded a blue needles of suitable quality for X-ray crystallography. Melting point 200 °C. *Anal.* Calc. for $C_{16}H_{18}N_4O_8Cl_2Cu$: C, 36.34; H, 3.34; N, 10.59. Found: C,36.11; H, 3.19; N, 10.59%. Λ_M (S cm^2 mol^{-1} in CH_3CN) and CH_3NO_2: 270 and 133. IR (cm^{-1}): υ(N–H) 3300, 3255, 3158; υ(C=N) 1636; υ(C=C), υ(C=N)$_{py}$, δ(N–H) 1598, 1580; υ(ClO_4) 1053. UV–Vis (CH_3CN; λ_{max}): 606, 412 nm. μ_{eff} (BM): 1.75.

2.4.4. [CuL(N$_3$)][NO$_3$] (**5**)

An ethanolic solution (12 cm^3) of $Cu(NO_3)_26H_2O$ (2.2 g, 0.01 mol) was added dropwise to ethanolic solution (10 cm^3) of (**1**) (1.0 g, 0.0044 mol) with continuous stirring. The reaction mixture was stirred for one hour and the solution changed colour to a greenish-blue. To this NaN_3 (1.2 g, 0.02 mol) in hot methanol (15 cm^3) was added slowly with constant stirring. The colour changed immediately and a brown precipitate formed. The reaction mixture was stirred for 3 h. at room temperature, the precipitate was filtered, washed with few drops of ethanol and dried under vacuum. This precipitate was disgraded (as it proved to be a mixture). The green filtrate was concentrated using a rotary evaporator and kept at 4 °C in a fridge for several weeks. Unusual dark green spherical pseudo-crystals (unsuitable for crystallography) were isolated, washed with few drops of ethanol and dried under vacuum. Melting point 115 °C. *Anal.* Calc. for $C_{14}H_{15}N_7O_3Cu$: C, 42.8; H, 3.84; N, 24.96. Found: C, 42.32; H, 3.10; N, 25.09%. Λ_M (S cm^2 mol^{-1}) in CH_3CN and CH_3NO_2: 128 and 68. IR (cm^{-1}): υ(N–H) 3292, 3244, 151; υ(N_3) 2042; υ(C=N) 1660, 1636; υ(C=C), υ(C=N)$_{py}$, δ(N–H) 1594, υ(NO_3) 1411. UV–Vis (CH_3CN; λ_{max}): 614, 518 nm. μ_{eff} (BM): 1.74.

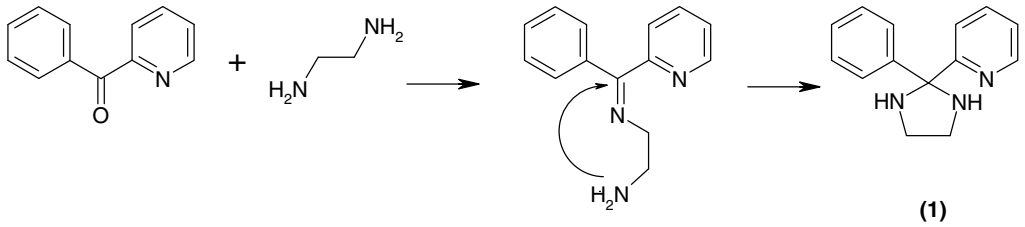

(1)

Scheme 1.

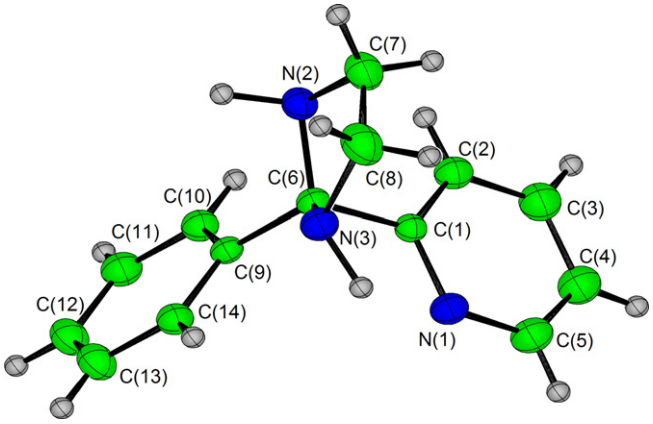

Fig. 1. ORTEX diagram of $C_{14}H_{15}N_3$, L (**1**) with 40% probability ellipsoids.

2.4.5. $[CuL(H_2O)][NO_3]_2$ (**6**)

The filtrate remaining after the filtration of (**5**) was left to stand at room temperature for several weeks and a precipitate formed. This was isolated by filtration, and washed with few drops of ethanol and crystallized from methanol solution and dark blue crystals were grown by slow vapour diffusion of diethyl ether from an adjacent container which were suitable for X-ray crystallography. Melting point 135 °C. *Anal.* Calc. for $C_{14}H_{17}N_5O_7Cu$ (**6**): C, 39.03; H, 3.97; N, 16.25. Found: C, 38.49; H, 4.01; N, 15.23%. Λ_M ($S\,cm^2\,mol^{-1}$) in CH_3CN and CH_3NO_2: 141 and 50. IR (cm^{-1}): υ(O–H) 3400–2327; υ(N–H) 3293, 3240,3135; υ(C=N) 1645; 1597, 1585; $\upsilon(NO_3)$ 1411. UV–Vis (CH_3CN; λ_{max}): 648, 516 nm. μ_{eff} (BM): 1.76.

2.4.6. $[CuL(N_3)][ClO_4]$ (**7**)

A blue methanolic solution (7 cm^3) of $Cu(ClO_4)_2 \cdot 6H_2O$ (1.6 g, 0.004 mol) was added dropwise to a methanolic solution (7 cm^3) of **L** (0.5 g, 0.002 mol) with continuous stirring. The mixture was stirred for 20 min and then NaN_3 (0.6 g, 0.01 mol) in aqueous methanol (10 cm^3, 1:1) was added slowly with a constant stirring. The blue colour of the reaction mixture changed to dark brown with the formation of green precipitate. This was filtered off washed with methanol and dried. It was re-crystallized from hot acetonitrile to give blue crystals which were suitable for crystallography. Its melting point is 175 °C. *Anal.* Calc. for $C_{14}H_{15}N_6O_4ClCu$ (**7**): C, 39.07; H, 3.51; N, 39.53. Found: C,39.27; H, 2.99; N, 19.45%. (Λ_M $S\,cm^2\,mol^{-1}$) in CH_3CN CH_3NO2: 153 and 104. IR (cm^{-1}): υ(N–H) 3317, 3264, 3148; υ(C=N) 1649; 1598, 1585; $\upsilon(ClO_4)$ 1096. UV–Vis (CH_3CN; λ_{max}): 611, 513 nm. μ_{eff} (BM): 1.80.

2.4.7. $[Cu_2(L)_2(Pyz)][ClO_4]_4\ CH_3CN \cdot (H_2O)_{0.5}$ (**8**)

To a solution of (**1**) (1.0 g, 0.004 mol) in C_2H_5OH (10 cm^3) was added solution of $Cu(ClO_4)_26H_2O$ (3.3 g, 0.004 mol) in water (5 cm^3). The solution colour changed from yellow to blue and the reaction mixture was then stirred for 30 min. at room temperature. To this pyrazine (1.4 g, 0.02 mol) in water (5 cm^3) was added slowly with constant stirring. After stirring at room temperature for 5 h the solution was allowed to stand and a precipitate was filtered, washed with ethanol and dried under vacuum over P_2O_5. It was crystallized from a mixture of CH_3CN and CH_3OH (1:3) by slow vapour diffusion of diethyl ether from an adjacent container giving dark violet crystals which were not suitable for X-ray crystallography. Melting point 140 °C. *Anal.* Calc. for $C_{34}H_{38}N_9O_{16.5}Cl_4Cu_2$ (**8**): C, 36.93; H, 3.46; N, 11.49. Found (>250 °C): C, 37.12; H, 3.36, N, 10.54%. Λ_M ($S\,cm^2\,mol^{-1}$) in CH_3CN: 507. IR (cm^{-1}): υ(O–H) 3567, 3407; υ(N–H) 3316, 3260, 3140; υ(C=N) 1649; υ(C=C), $\upsilon(C{=}N)_{py}$

Table 1
Crystal data and structure refinement parameters

Compound	(**1**)	(**2**)	(**4**)	(**6**)	(**7**)
Empirical formula	$C_{14}H_{15}N_3$	$C_{29}H_{31}Cl_5N_6NiO_8$	$C_{16}H_{18}Cl_2CuN_4O_8$	$C_{14}H_{17}CuN_5O_7$	$C_{14}H_{15}ClCuN_6O_4$
Formula weight	225.29	827.56	528.78	430.87	430.31
Temperature (K)	298(2)	298(2)	150(2)	298(2)	150(2)
Wavelength (Å)	0.71069	0.71069	0.71073	0.71069	0.71073
Crystal system	monoclinic	monoclinic	orthorhombic	monoclinic	monoclinic
Space group	*C2/c*	*P21/c*	*Pbca*	*P21/c*	*C2/c*
Unit cell dimensions					
a (Å)	16.690(2)	15.097(2)	7.14000(10)	8.486(2)	24.6030(8)
b (Å)	5.796(1)	25.636(3)	22.8780(2)	23.617(3)	8.2460(3)
c (Å)	24.465(3)	18.197(2) $\gamma = 90°$	25.5040(3)	8.7509(9)	17.1500(7)
β (°)	95.25(2)	90.74(2)		92.130(10)	106.7130(10)
Volume ($Å^3$)	2356.7(6)	7042.1(15)	4166.05(8)	1752.6(5)	3332.4(2)
Z	8	8	8	4	8
Density (calculated) (Mg/m^3)	1.270	1.561	1.686	1.633	1.715
Absorption coefficient (mm^{-1})	0.078	0.987	1.358	1.296	1.507
F(000)	960	3392	2152	884	1752
Crystal size (mm)	0.55 × 0.42 × 0.26	0.47 × 0.38 × 0.21	0.40 × 0.20 × 0.10	0.47 × 0.41 × 0.26	0.10 × 0.05 × 0.05
θ Range for data collection (°)	1.67–20.34	1.57–20.52	3.56–27.46	1.72–20.43	4.98–27.47
Index ranges	$-16 \leqslant h \leqslant 15$; $-5 \leqslant k <= 5$; $-23 \leqslant l \leqslant 23$	$-14 \leqslant h \leqslant 14$; $-23 \leqslant k <= 24$; $-17 \leqslant l \leqslant 17$	$-9 \leqslant h \leqslant 9$; $-29 \leqslant k \leqslant 29$; $-33 \leqslant l \leqslant 33$	$-7 \leqslant h <= 7$; $-22 \leqslant k \leqslant 22$; $-8 \leqslant l \leqslant 8$	$-31 \leqslant h <= 31$; $-8 \leqslant k \leqslant 10$; $-22 \leqslant l \leqslant 21$
Reflections collected	4312	22 309	58 203	6763	11 733
Independent reflections [*R*(int)]	1137 [0.0361]	6869 [0.0367]	4751 [0.0732]	1639 [0.0528]	3679 [0.0781]
Reflections observed (>2σ)	1091	6306	3514	1566	2583
Data completeness	0.977	0.972	0.997	0.941	0.964
Absorption correction	none	none	none	none	none
Data/restraints/parameters	1137/0/157	6869/0/883	4751/2/307	1639/0/245	3679/2/243
Goodness-of-fit on F^2	1.066	1.036	1.028	1.094	1.022
Final *R* indices [$I > 2\sigma(I)$]	$R_1 = 0.0363$ $wR_2 = 0.1029$	$R_1 = 0.0656$ $wR_2 = 0.1743$	$R_1 = 0.0377$ $wR_2 = 0.0846$	$R_1 = 0.0467$ $wR_2 = 0.1247$	$R_1 = 0.0437$ $wR_2 = 0.0843$
R indices (all data)	$R_1 = 0.0387$ $wR_2 = 0.1046$	$R_1 = 0.0706$ $wR_2 = 0.1786$	$R_1 = 0.0619$ $wR_2 = 0.0948$	$R_1 = 0.0523$ $wR_2 = 0.1410$	$R_1 = 0.0784$ $wR_2 = 0.0987$
Largest difference peak and hole (e $Å^{-3}$)	0.130 and −0.136	1.158 and −0.811	0.419 and −0.457	0.781 and −0.474	0.365 and −0.467

Table 2
Selected bond lengths (Å) and angles (°) for (**1**)

N(2)–C(6)	1.466(3)	N(2)–C(7)	1.468(3)
N(3)–C(8)	1.465(3)	N(3)–C(6)	1.480(2)
C(6)–C(9)	1.520(3)	C(1)–C(6)	1.540(3)
C(6)–C(9)	1.520(3)	C(7)–C(8)	1.510(3)
C(1)–C(6)–C(9)	107.5(2)	C(6)–N(3)–C(8)	106.1(2)
C(6)–N(2)–C(7)	103.3(2)	N(2)–C(7)–C(8)	105.8(2)
N(3)–C(8)–C(7)	105.9(2)	C(1)–C(6)–N(2)	109.6(2)

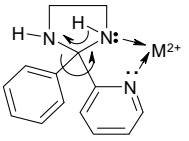

Fig. 2. Metal induced ring opening of the imadazoline.

δ(N–H) 1600, 1567; $\upsilon(ClO_4)$ 1095, 1043. UV–Vis (CH_3CN; λ_{max}): 650, 512 nm. μ_{eff} (BM): 1.09.

2.5. Crystallography

Reflection data were collected either on a Marresearch image plate system or on a Nonius kappa CCD system. Data reduction were carried out using the XDS and DENZO/SCALEPACK packages. respectively [8] The structures was solved by direct methods, SHELXS-97, and refined by full matrix least squares using SHELXL-97 [9,10]. SHELX operations were automated using ORTEX which was also used to obtain the drawings [11]. Hydrogen atoms were included in calculated positions with thermal parameters 30% larger than the atom to which they were attached. The non-hydrogen atoms were refined anisotropically. All calculations were performed on a Pentium PC.

2.6. Calculations

DFT calculations were carried out using PC-GAMESS [12] which was driven by the molecular modeling software within the OSCAIL package [13].

3. Results and discussion

3.1. Structure of the ligand

The condensation of 2-benzoyl pyridine and 1,2-diaminoethane has been reported and the structure of the product assigned as 2-

Table 3
Selected bond lengths (Å) and angles (°) for (**2**)

Ni(1)–N(1)	2.121(5)	Ni(1)–N(2)	1.996(5)
Ni(1)–N(3)	2.103(5)	Ni(1)–N(4)	2.112(5)
Ni(1)–N(5)	2.016(5)	Ni(1)–N(6)	2.093(5)
Ni(2)–N(7)	2.121(5)	Ni(2)–N(8)	1.998(5)
Ni(2)–N(9)	2.095(5)	Ni(2)–N(10)	2.115(5)
Ni(2)–N(11)	2.017(5)	Ni(2)–N(12)	2.088(5)
N(1)–Ni(1)–N(2)	81.4(2)	N(1)–Ni(1)–N(3)	158.4(2)
N(1)–Ni(1)–N(4)	92.1(2)	N(1)–Ni(1)–N(5)	100.7(2)
N(1)–Ni(1)–N(6)	89.5(2)	N(7)–Ni(2)–N(8)	80.5(2)
N(7)–Ni(2)–N(9)	158.3(2)	N(7)–Ni(2)–N(10)	90.7(2)
N(7)–Ni(2)–N(11)	101.6(2)	N(7)–Ni(2)–N(12)	91.0(2)

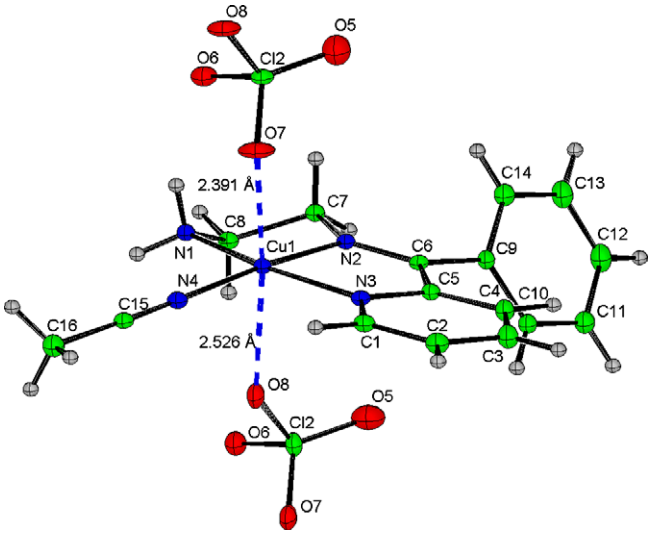

Fig. 4. ORTEX diagram of $[CuL(CH_3CN)][ClO_4]_2$ (**4**), with 40% probability ellipsoids.

Table 4
Selected bond lengths (Å) and angles (°) for (**4**)

Cu(1)–N(1)	2.008(2)	Cu(1)–N(2)	1.957(2)
Cu(1)–N(3)	1.996(2)	Cu(1)–N(4)	1.983(2)
Cu(1)–O(7)	2.391(2)	N(1)–Cu(1)–N(2)	83.51(9)
N(1)–Cu(1)–N(3)	163.95(9)	N(1)–Cu(1)–N(4)	96.37(9)
N(2)–Cu(1)–N(3)	80.77(8)	N(2)–Cu(1)–N(4)	174.70(8)
N(3)–Cu(1)–N(4)	98.98(8)	N(1)–Cu(1)–O(7)	92.15(8)
N(2)–Cu(1)–O(7)	97.87(9)	N(3)–Cu(1)–O(7)	93.20(8)
N(4)–Cu(1)–O(7)	87.43(9)		

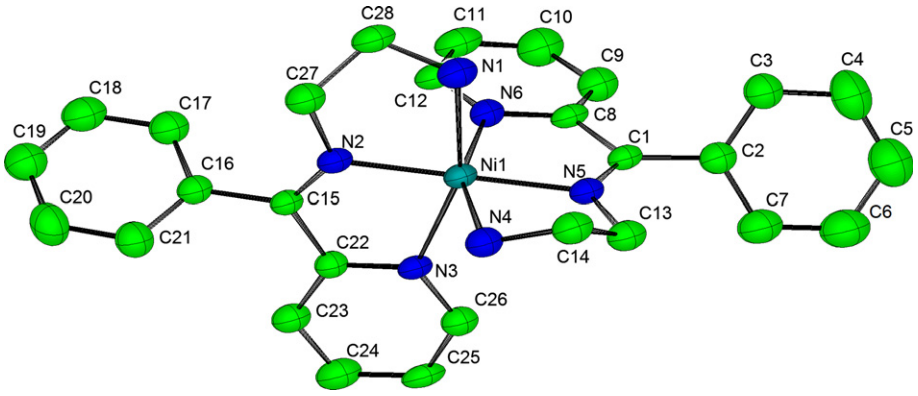

Fig. 3. ORTEX diagram of the cation of $[NiL_2][ClO_4]_2$ (**2**) with 40% probability ellipsoids and hydrogen atoms omitted for clarity.

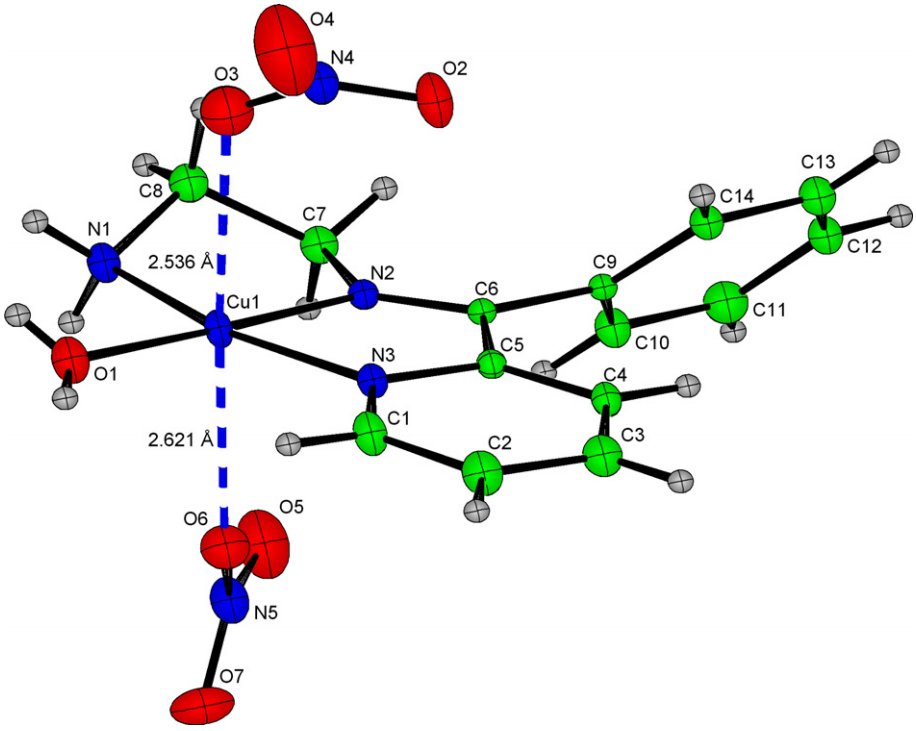

Fig. 5. ORTEX diagram of the cation of $[Cu(L)(H_2O)][(NO_3)_2]$ (**6**), with 40% probability ellipsoids.

Table 5
Selected bond lengths (Å) and angles (°) for (**6**)

Cu(1)–O(1)	1.942(5)	Cu(1)–N(2)	1.948(5)
Cu(1)–N(1)	1.994(5)	Cu(1)–N(3)	2.003(5)
Cu(1)–O(3)	2.621(6)	Cu(1)–O(6)	2.536(5)
N(1)–Cu(1)–N(2)	84.2(2)	N(1)–Cu(1)–N(3)	164.9(2)
N(2)–Cu(1)–N(3)	80.8(2)	O(1)–Cu(1)–N(1)	93.9(2)
O(1)–Cu(1)–N(2)	178.0(2)	O(1)–Cu(1)–N(3)	101.1(2)
O(3)–Cu(1)–O(6)	173.6(2)		

phenyl-2-(2-pyridyl)imidazolidine, (**1**), using ^{1}H and ^{13}C NMR. It is reasonable to suggest that the reaction proceeds *via* initial formation of the imine and subsequent cyclization as shown in Scheme 1.

Since this is an example of an unfavorable 5-*Endo-Trig* cyclization [4], the crystal structure was determined to confirm the NMR assignment. The X-ray structure of (**1**) is shown in Fig. 1.

Table 6
Selected bond lengths (Å) and angles (°) for (**7**)

Cu(1)–N(4)	1.946(3)	Cu(1)–N(2)	1.950(3)
Cu(1)–N(3)	2.010(3)	Cu(1)–N(1)	2.033(3)
N(1)–C(8)	1.494(4)	N(2)–C(6)	1.279(4)
N(2)–C(7)	1.466(4)	N(3)–C(1)	1.333(4)
N(3)–C(5)	1.364(4)	N(4)–N(5)	1.204(4)
N(5)–N(6)	1.162(4)	C(1)–C(2)	1.381(5)
C(2)–C(3)	1.382(5)	C(3)–C(4)	1.398(5)
C(4)–C(5)	1.384(5)	C(5)–C(6)	1.498(4)
C(6)–C(9)	1.491(4)	C(7)–C(8)	1.522(5)
N(4)–Cu(1)–N(2)	173.0(1)	N(4)–Cu(1)–N(3)	94.9(1)
N(2)–Cu(1)–N(3)	80.5(1)	N(4)–Cu(1)–N(1)	101.8(1)
N(2)–Cu(1)–N(1)	83.7(1)	N(3)–Cu(1)–N(1)	161.1(1)
C(8)–N(1)–Cu(1)	107.2(2)	C(6)–N(2)–C(7)	126.9(3)
C(6)–N(2)–Cu(1)	118.8(2)	C(7)–N(2)–Cu(1)	114.3(2)
C(1)–N(3)–C(5)	118.6(3)	C(1)–N(3)–Cu(1)	127.9(2)
C(5)–N(3)–Cu(1)	113.4(2)	N(5)–N(4)–Cu(1)	126.0(2)
N(6)–N(5)–N(4)	176.6(3)	N(3)–C(1)–C(2)	122.3(3)

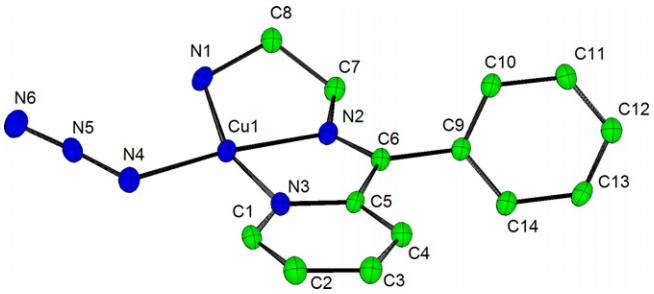

Fig. 6. ORTEX diagram of the cation of $[Cu(L)N_3][ClO_4]$ (**7**), with 40% probability ellipsoids and hydrogen atoms omitted for clarity.

Crystal data are given in Table 1 and selected bond lengths and angles are given in Table 2.

DFT calculations on (**1**) using B3LYP functionals at the 6-31G* level suggest that in the gas phase the cyclic structure is more stable than the open imine form by 13.1 kJ mol^{-1}. Thus the unfavourable 5-*Endo-Trig* cyclization may in part be possible in this case due to the higher stability of the cyclic form. If solvent effects are ignored, and if equilibrium was possible, this energy difference translates to an equilibrium concentration of the cyclic form that is approximately 5×10^3 times greater than the imine form. There is spectroscopic and kinetic evidence that the imine form may have appreciably higher concentrations in polar solvents [14]. There are many well established examples of 5-*Endo-Trig* cyclizations in the literature [15,16].

3.2. Ring opening complexation

When (**1**) was reacted with Cu(II) and Ni(II) salts no complexes containing the cyclic structure were observed. In every case where crystal structures were obtained only the open form was observed in the complexes. This reaction is probably an example of a cationic

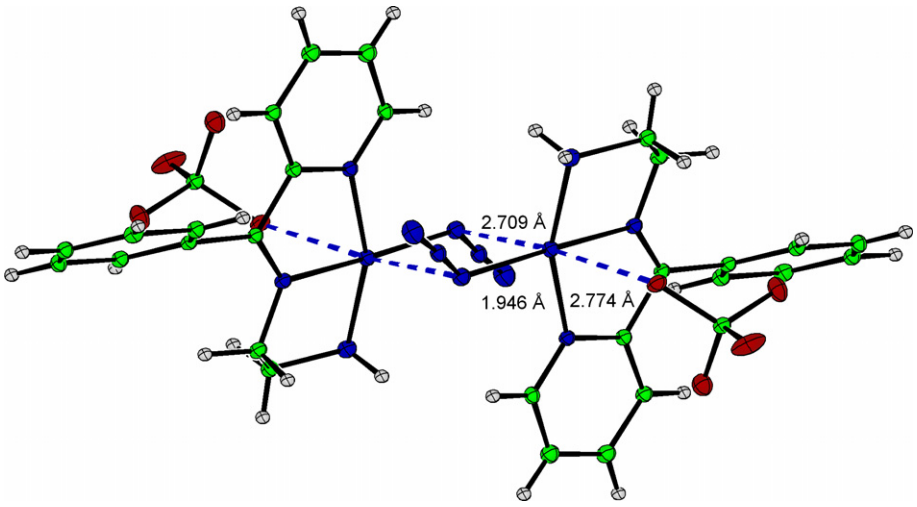

Fig. 7. ORTEX diagram of showing the weak interactions in the crystal structure of (**7**).

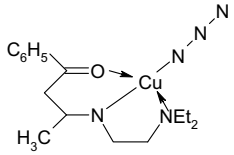

Fig. 8. Structure of (**8**).

metal induced ring opening reaction. A possible mechanism is illustrated in Fig. 2.

This mechanism is related to that proposed for the Fe(III) catalysed opening of an imidazolidine ring in the presence of alcohols [17].

3.3. Reaction of (*1*) with nickel perchlorate (*2*)

Reaction of (**1**) with nickel perchlorate led to the isolation of a red solid. It was characterized by elemental analysis, IR and ^{1}H and ^{13}C NMR. Crystals grown from a chloroform/methanol mixture were suitable for X-ray crystallography. The structure of a cation from the crystal structure of (**2**) is shown in Fig. 3. Crystal data are given in Table 1 and selected bond lengths and angles are given in Table 3. There are two almost identical formula units in the crystallographic asymmetric unit. Each of the ligands in the cation is tridentate with and the overall geometry is close to octahedral. Thus within each asymmetric unit there are four examples of nickel ligand binding moeties. The nickel–nitrogen distances in all cases are in order of increasing length; imine, pyridine and primary amine. For example in Fig. 3 the Ni(1)–N(2), Ni(1)–N(3) and Ni(1)–N(1) are 1.996(5), 2.103(5) and 2.121(5) Å.

To see if this order of bond lengths was due to crystal packing or a genuine property of the complex the structure of the cation was optimized using DFT calculations using B3LYP functionals at the 6-31G* level [12]. The results while giving slightly longer distances nevertheless gave the same order of bond lengths; N-i-N(2) 2.040, Ni–N(3) 2.115 and Ni–(N1) 2.183 Å. The bonding to nickel on the part of the unsaturated nitrogens is clearly stronger than that of the primary nitrogen. It is possible that a small amount of strain in the chelate rings is the cause of the shortest Ni–N bond being to the middle nitrogen. The observed magnetic moment of 3.34 μB is higher that the spin-only value for two unpaired electrons of 2.83 μB however it is within the observed range for octahedral nickel(II) complexes [18,19].

3.4. Reaction of (*2*) with sodium azide

When complex (**2**) was reacted with sodium azide a product of formula $[Ni(L)(N_3)_2(DMF)]$ (**3**) was isolated. Single crystals suitable for X-ray crystallography could not be obtained. This formula is assigned on the basis of elemental analysis, spectroscopic, magnetic and conductivity data. In the IR spectrum bands due to azide, DMF and the Schiff base were all observed. The observed conductivity is an order of magnitude lower than that observed for (**2**) in agreement with its covalent formulation.

3.5. Reaction of (*1*) with copper nitrate and acetonitrile in methanol

Treatment of a solution of (**1**) in methanol with copper perchlorate gave a blue solution from which after addition of acetonitrile blue crystals of formula $[CuL(CH_3CN)][ClO_4]_2$ (**4**) were obtained. The structure of a cation from (**4**) and its contacts to one of the perchlorate anions is shown in Fig. 4, crystal data are in Table 1 and selected bond distances and angles are given in Table 4. The geometry about copper is tetragonally distorted octahedral with metal nitrogen distances within the square plane close to 2.0 Å and longer contacts to the oxygen atoms of symmetry related perchlorate anions of 2.391(2) and 2.526(2) Å, respectively. The metal nitrogen bond lengths within the salicylaldimine ligand show the same order observed in the nickel complex (**2**) above.

3.6. Reaction of (*1*) with copper nitrate and sodium azide in ethanol

An ethanolic solution of copper nitrate was reacted with (**1**) and sodium azide. On standing for some time tiny green spheres grew from solution. These spheres did not diffract X-rays and they had the properties of a glass. The formula $[CuLN_3][NO_3]$ (**5**) was assigned to this solid on the basis of analytical and spectroscopic data. Attempts to grow crystals from the filtrate of this reaction led to the isolation of crystals of $[Cu(L)(H_2O)][(NO_3)_2]$ (**6**), in which water had replaced the azide anion. The structure of the cation from (**6**) is shown in Fig. 5, crystal data are given in Table 1 and selected bond lengths and angles are given in Table 5. The geometry about the copper is tetragonally distorted octahedral with longer contacts to nitrate oxygens. The coordinated water molecule is involved in strong hydrogen bond contacts to nitrate ions, O···O distances of 2.739(7) and 2.763(7) Å to O6 and O3, respectively, and there are contacts from nitrate O7 to N1 of 3.078(7) Å which extend the hydrogen bond network throughout the lattice.

When weak interactions are included the stereochemistry of the copper(II) ion is often difficult to describe due to the distortions resulting from the Jahn–Teller effect. In an extensive review of this area using structure correlation analysis Murphy and Hathaway have analysed the range of observed structures and the crystal structure of (**5**) lies well within that range [20]. Attempts were made to model the strongly bonded square planar portion of the structure using the DFT calculation methods that had been successfully applied to the nickel complex above. In the crystal structure of (**6**) the copper and the three nitrogen atoms are essentially planar, with a maximum deviation from least squares plane of 0.02 Å. The oxygen atom is just 0.10 Å above this plane. In the DFT optimised structure the maximum deviation from the plane defined by the copper and the three nitrogens is 0.18 Å and the oxygen is 1.12 Å out of that plane. Attempts to model the complete $[Cu(L)(H_2O)][(NO_3)_2]$ unit were even less successful. The B3LYP functional appears to be able to model Cu(II) when the relative geometry of the ligating atoms is restrained to some extent [5,6]. A recent review of DFT functionals has suggested that B3LYP has some serious shortcomings and perhaps more advanced functionals are required for the Cu(II) complexes described here [21].

3.7. Reaction of (*1*) with copper perchlorate and sodium azide in methanol

When the reaction above was repeated using copper perchlorate in methanol solution it was possible to isolate good quality crystals of the copper azide $[Cu(L)N_3][ClO_4]$ (**7**). Crystal data are given in Table 1 and selected bond lengths and angles are in Table 6. The crystal structure of the cation from this salt without the weaker interactions which complete the tetragonally distorted octahedral geometry is shown in Fig. 6.

The geometry about the copper is close to square-planar with N2 showing the greatest deviation from the best plane through the four nitrogens of 0.15 Å and the copper is 0.04 Å out of the plane. The tetragonally distorted octahedral geometry about copper is achieved by the addition of two weak interactions involving highly asymmetric bridging on the part of the azide ligands, 1.946(3) and 2.709(3) and a weak interaction involving a perchlorate anion, 2.774(3) Å (Fig. 7).

There are many reported structures of azide complexes in which the azide ligand is seen to span the range from mono-dentate through semi-bridging to symmetrical bridging. Structure (**7**) is close to mono-dentate. The energy difference between mono-dentate and bridging structures is however small and less than typical lattice energies. This point is clearly evident in the recently reported structure of complex (**8**), depicted in Fig. 8, which Sarker et al. have described [22,23]. In the reported crystal structure both symmetrically bridged μ-azido and mono-dentate square-planar geometries are present in the same asymmetric unit.

4. Conclusion

2-Phenyl-2-(2-pyridyl)imidazolidine reacts with Ni(II) and Cu(II) salts to give stable complexes containing the tridentate open form of the ligand. Combined structural and theoretical calculations show that DFT calculations using the B3LYP functionals at the 6-31G* level reproduce the geometry of the Ni(II) complexes but are less successful in modelling the Cu(II) complexes.

Appendix A. Supplementary data

CCDC 677183, 677184, 677185, 677186 and 677187 contain the supplementary crystallographic data for **1**, **2**, **4**, **6** and **7**. These data can be obtained free of charge via http://www.ccdc.cam.ac.uk/conts/retrieving.html, or from the Cambridge Crystallographic Data Centre, 12 Union Road, Cambridge CB2 1EZ, UK; fax: (+44) 1223-336-033, or e-mail: deposit@ccdc.cam.ac.uk. Supplementary data associated with this article can be found, in the online version, at doi:10.1016/j.poly.2008.04.028.

References

[1] D. Shi, Z. You, C. Xu, Q. Zhang, H. Zhu, Inorg. Chem. Commun. 10 (2007) 404.
[2] C.M. Sharaby, Spectrochim. Acta A 66 (2007) 127.
[3] C. Jin, W. Fan, Y. Jia, B. Fan, J. Ma, R. Li, J. Mol. Cat. A: Chem. 249 (2006) 23.
[4] J.E. Baldwin, J. Chem. Soc., Chem. Commun. (1976) 734.
[5] V. Ruangpornvisuti, Struct. Chem. 18 (2007) 977.
[6] S. Ritimukta, S.I. Gorelsky, L. Basumallick, H.J. Hwang, R.C. Pratt, T.D.P. Stack, Y. Lu, K.O. Hodgson, B. Hedman, E.I. Solomon, J. Am. Chem. Soc. 130 (2008) 3866.
[7] H. Sharghi, H. Naeimi, Synlett 12 (1998) 1343.
[8] (a) XDS, W. Kabasch, J. Appl. Crystallogr. 21 (1988) 916;
(b) Denzo/Scalepack, Z. Otwinowski, W. Minor, International Tables for Crystallography, vol. F, Springer, 2001.
[9] G.M. Sheldrick, Acta Crystallogr., Sect. A 46 (1990) 467.
[10] G.M. Sheldrick, SHELXL-97 A Computer Program for Crystal Structure Determination, University of Gottingen, 1997.
[11] P. McArdle, J. Appl. Crystallogr. 28 (1995) 65.
[12] PC GAMESS program provided by A.A. Granovsky, PC GAMESS version 7.1.5, <http://classic.chem.msu.su/gran/gamess/index.html>.
[13] P. McArdle, K. Gilligan, D. Cunningham, R. Dark, M. Mahon, CrystEngComm 6 (2004) 303.
[14] J. McManus, M.J. Hynes, unpublished observations.
[15] A. Ishita, O. Tamura, Tetrahedron Lett. 43 (2002) 473.
[16] T. Yamazaki', S. Hiraoka, J. Sakamoto, T. Kitazume, J. Fluorine Chem. 101 (2000) 309.
[17] V.M. Ugalde-Saldivar, H. Hopfl, N. Farfan, A.R. Toscano, M.E. Sosa-Torres, Inorg. Chim. Acta 358 (2005) 3545.
[18] C.E. Housecroft, A.G. Sharpe, Inorganic Chemistry, 3rd ed., Pearson, Harlow, 2008, p. 672.
[19] F.A. Cotton, G. Wilkinson, C.A. Murillo, M. Bochmann, Advanced Inorganic Chemistry, 6th ed., Wiley, New York, 1999. p. 839.
[20] B. Murphy, B. Hathaway, Coord. Chem. Rev. 243 (2003) 237.
[21] Y. Zhao, D.G. Truhlar, Acc. Chem. Res. 41 (2008) 157.
[22] B. Sarkar, M.S. Ray, M.G.B. Drew, C. Lu, A. Ghosh, J. Coord.Chem. 60 (2007) 2165.
[23] F.H. Allen, Acta Crystallogr., Sect. B 58 (2002) 380.